Pathology - Research and Practice 215 (2019) 159–170

Contents lists available at ScienceDirect

Pathology - Research and Practice

journal homepage: www.elsevier.com/locate/prp

Comprehensive analysis of tumor immune infiltration associated with endogenous competitive RNA networks in lung adenocarcinoma

Boyang Wei[a], Wei Kong[a,*], Xiaoyang Mou[b], Shuaiqun Wang[a]

[a] College of Information Engineering, Shanghai Maritime University 1550 Haigang Ave., Shanghai, 201306, PR China
[b] Department of Biochemistry, Rowan University and Guava Medicine Glassboro, NJ, 08028, USA

ARTICLE INFO

Keywords:
Competitive endogenous RNA
Immunogenomics
Lung adenocarcinoma
Genomics
Cancer immunotherapy

ABSTRACT

Cancer immunotherapy has achieved unprecedented success in the treatment of cancer. However, different patients have different responses to immunotherapy. More and more studies have shown that tumor immune heterogeneity has an important influence on the prognosis of cancer. Therefore, understanding the clinical impact of tumor immune infiltration and the regulatory mechanism of RNA molecules is crucial for exploring the pathogenesis of lung adenocarcinoma (LUAD) and the development of immunotherapy protocols.The endogenous competitive RNA hypothesis provides new ideas for studying immune heterogeneity. Therefore, by using the method of immune genomics, this article explores the relationship between immune infiltration and prognosis of patients with lung adenocarcinoma, and found that B-cell immune infiltration highly affects the survival of patients. Through differential analysis, differential mRNAs, lncRNAs and miRNAs were extracted, and 318 differentially expressed mRNAs related to B cell immunity were screened by correlation analysis, and prognosis of patients with COX risk regression model was predicted and analyzed. Through multiple database searches, an immune-related ceRNA regulatory network was constructed, containing 3 key mRNAs, 4 miRNAs, and 50 lncRNAs. Three mRNAs and most miRNAs, lncRNAs, are significantly associated with LUAD prognosis. Bioinformatics analysis of the network showed that *LINC*00337 may up-regulate the expression of *PBK* and *KIF23* through competitive binding of *has-mir-373* and *has-mir-519d*. The competitive binding of *has-mir-373* and *has-mir-372* can up-regulate the expression of *SLC7A11*. The interaction between these RNAs may have an important regulatory role in the immune infiltration in lung adenocarcinoma, thereby affecting the patient's prognosis and immunotherapy efficacy.

1. Introduction

In recent years, there have been several breakthrough advances in tumor immunotherapy technologies for lung cancer [1,2], such as blockade of immune checkpoint therapy to improve anti-tumor immune response by regulating T cell activity. However, due to the off-target effect, tumor microenvironment heterogeneity and immunosuppression, immunotherapy still has some limitations in clinical application [3,4]. Therefore, researches from the point of view of tumor immunogenomics can enhance our comprehension of the tumor immune mechanism, then make a certain pre-judgment on the efficacy of immunotherapy.

In studies of tumor immunogenomics, assessment of tumor immune infiltrating cells plays a key role in exploring how the interaction between the tumor and the immune system affects patient outcomes [5]. In this area of research, in addition to the traditional methods of chemical testing, many new calculation methods can improve our understanding of tumor microenvironment. Rooney et al. used a large-scale genomic dataset of a solid tissue tumor biopsy to quantify the cytolytic activity of local immune infiltration and identified the relevant characteristics of 18 tumor types [6]. Many recent studies have used label-based genes to infer subpopulation abundance of tumor immune cells [7–10]. CIBERSORT inferred the abundance of immuno-invasive components in 22 different tumors by referring to gene expression signature matrices and machine learning-based methods [9]. Although CIBERSORT is superior to other algorithms in eliminating noise, estimating the content of unknown mixtures, and accuracy, CIBERSORT can easily bias estimates due to the statistical collinearity effect produced by regression analysis. And this method is only applicable to microarray data, and RNA-Seq data of TCGA cannot be analyzed. The TIMER algorithm developed by LIBO et al. can detect and quantify the infiltration abundance of six immune cells in tumor tissues

* Corresponding author.
E-mail address: weikong@shmtu.edu.cn (W. Kong).

https://doi.org/10.1016/j.prp.2018.10.032
Received 13 July 2018; Received in revised form 13 October 2018; Accepted 26 October 2018

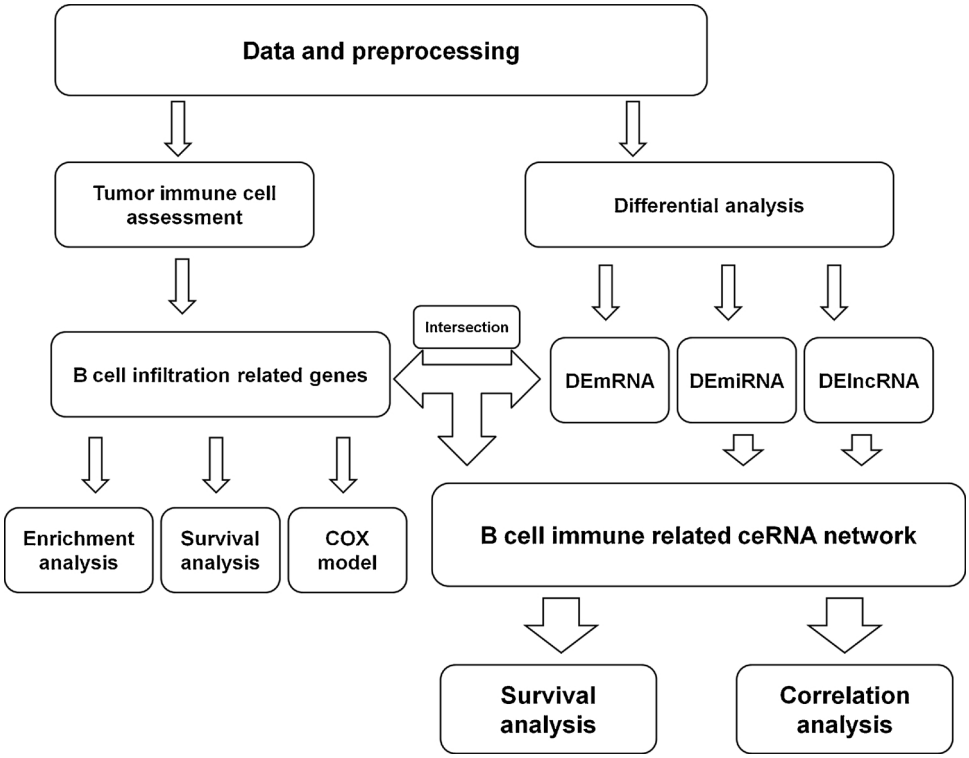

Fig. 1. General Research Framework.

from RNA-Seq expression profile data [8]. TIMER screens immune tag genes and removes highly expressed genes to eliminate bias effects, and can eliminate collinearity between immune cells to ensure inference accuracy. Therefore, our study selected the TIMER algorithm as the basis for exploring the immunoregulatory mechanism of LUAD.

In order to further explore the relationship between immune infiltration and cancer, the mechanism of immune heterogeneity is crucial from the perspective of RNA molecules. The discovery of Long noncoding RNA (lncRNA) provides a new perspective for genetic regulation of different biological environments. LncRNAs are novel heterologous non-coding RNAs that regulate gene expression and play an important role in cell differentiation and development [11]. Activation of immune cells is associated with dynamic changes in gene expression, and expression products of related genes can promote inflammatory responses in cells and tissues to initiate repair processes and promote repair. Recent evidence indicates that lncRNAs play an important role in directing the development of various immune cells and controlling dynamic transcriptional programs and are hallmarks of immune cell activation [12]. Salmena et al. In 2011, the competitive endogenous RNA (ceRNA) hypothesis was proposed [13]. This hypothesis proposes a new inter-genomic regulation method and plays an important role in the development of physiology and disease. MicroRNAs are known to cause gene silencing by binding to mRNA, while ceRNAs can regulate gene expression by competitively binding to microRNAs. ceRNA can interact with microRNAs through microRNA response elements (MREs) to affect microRNA-induced gene silencing, revealing the existence of an RNA- > microRNA regulatory pathway with significant biological significance. RNAs, pseudogenes, lncRNAs, circular RNAs, miRNAs, and other types of RNA can communicate with each other through ceRNA mechanisms to regulate a variety of tumor cells and their microenvironments and affect the proliferation and migration of tumors [12]. The ceRNA hypothesis provides us with a new way of exploring the molecular mechanisms of tumor immunity at the RNA level.

This study explored the relationship between immune infiltration and clinical LUAD, and studied the role of different RNAs in regulating LUAD immune response. We first used the TIMER algorithm to calculate the infiltration abundance of six immune cells in 594 LUAD samples from TCGA. Subsequently, through the survival analysis combined with clinical data and the construction of a regression model, we found that high infiltration of B cell predicts better survival of LUAD. Therefore, we selected mRNAs associated with B cell infiltration to investigate the relationship between B cell immune infiltration and RNA regulation in LUAD. Based on the ceRNA hypothesis, this study established a B cell immune-related ceRNA regulatory network. In the network, RNAs related to LUAD prognosis were excavated, the regulatory relationships between different RNAs were analyzed, and potential biomarkers for LUAD immunotherapy were searched. Our research provides new ideas for the study of immunotherapy.

2. Materials and methods

In this section, we describe the overall process of constructing a ceRNA network combined with tumor immunity (Fig. 1), and introduce the algorithms and bioinformatics analysis used in the study.

2.1. Data collection and preprocessing

LUAD transcriptome data, miRNA-Seq data and clinical data were downloaded from the TCGA database (https://cancergenome.nih.gov/). The transcriptome data included 594 samples (59 normal 535 tumors), and the miRNA-Seq data included 567 samples (46 normal 521 tumors). The download time is 2018.3.5. We deleted the data with a value of mostly zero and we used the RSEM-processed transcript per million (TPM) measure. For transcriptome data, we isolated lncRNA expression data and mRNA expression data for use in follow up research.

2.2. Differential expression analysis

For the cleaned raw data, differential RNA extraction was performed using the DESeq2 algorithm [14]. This method uses shrinkage estimation to spread and fold changes to improve the stability and

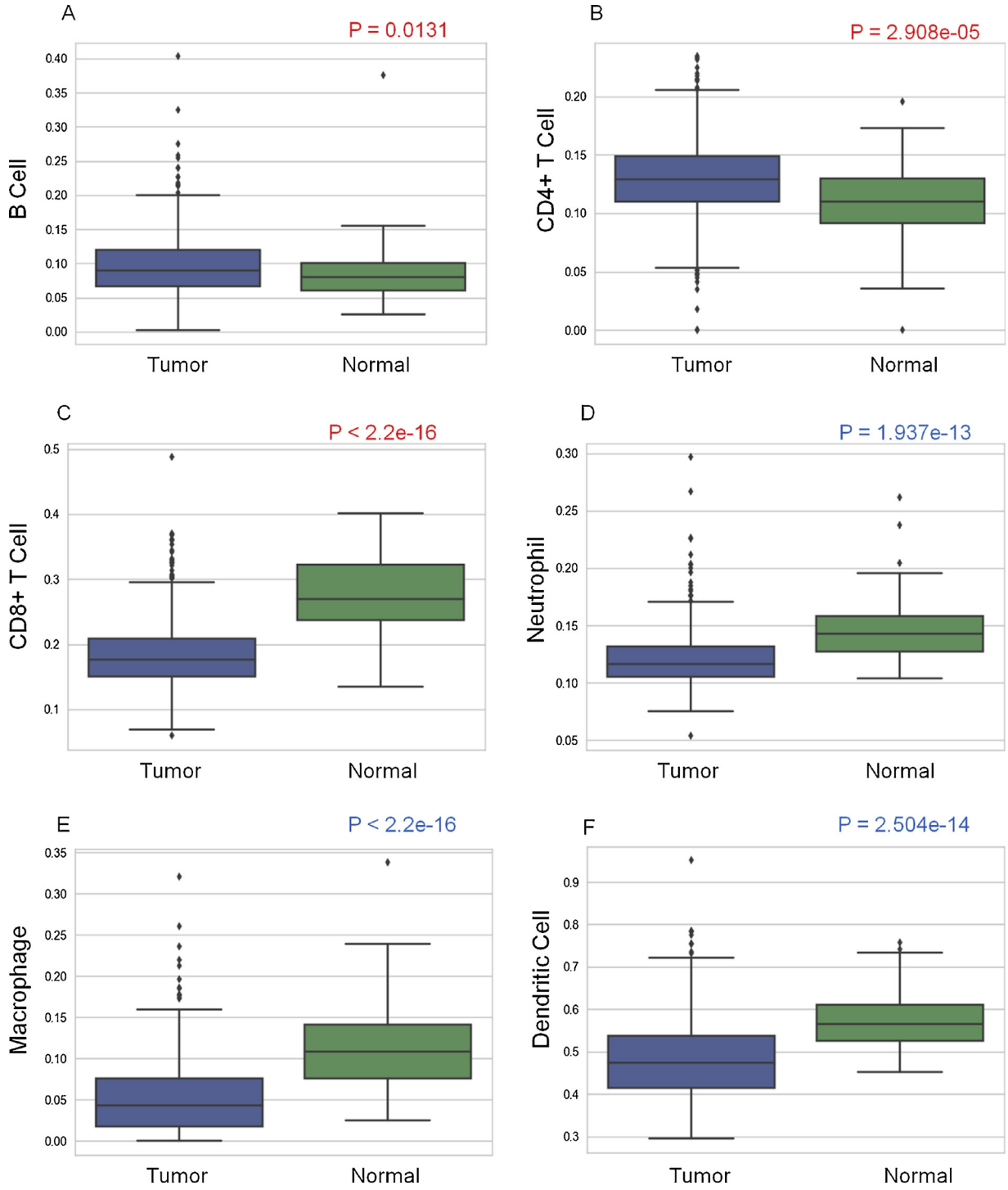

Fig. 2. Six immune cell infiltration abundances were significantly different in different tissue samples. Fig. 2A –F represents the distribution of the abundance of six immune cells (B cells, CD4 + T cells, CD8 + T cells, neutrophils, macrophages, and dendritic cells). Horizontal axis indicates sample type, vertical axis indicates immune cell type. Statistical significance was evaluated using the Wilcox rank-sum test, red as the infiltrate abundance was significantly elevated in tumor samples and blue was decreased (For interpretation of the references to colour in this figure legend, the reader is referred to the web version of this article).

interpretability of the DESeq-based estimation. We chose $|\log FC| > 2$, FDR < 0.05 as the threshold for screening differential genes. This process is implemented using the R package 'DESeq2'.

2.3. Immunocytotic infiltration abundance calculation method

The purpose of this study was to investigate the causes of tumor immunological heterogeneity and its relationship with prognosis. Therefore, it is important to calculate the abundance of immune cells in tumor samples. We use the TIMER algorithm developed by LIBO et al. to perform deconvolution calculations of immune cell components [8]. The TIMER algorithm first uses CHAT to estimate the tumor purity of each sample from the DNA SNP array data [15]. ComBat was then used to combine tumor gene expression with reference immune cell data for all genes, eliminating batch effects between different platform data [16]. Then, through correlation analysis, genes that are negatively

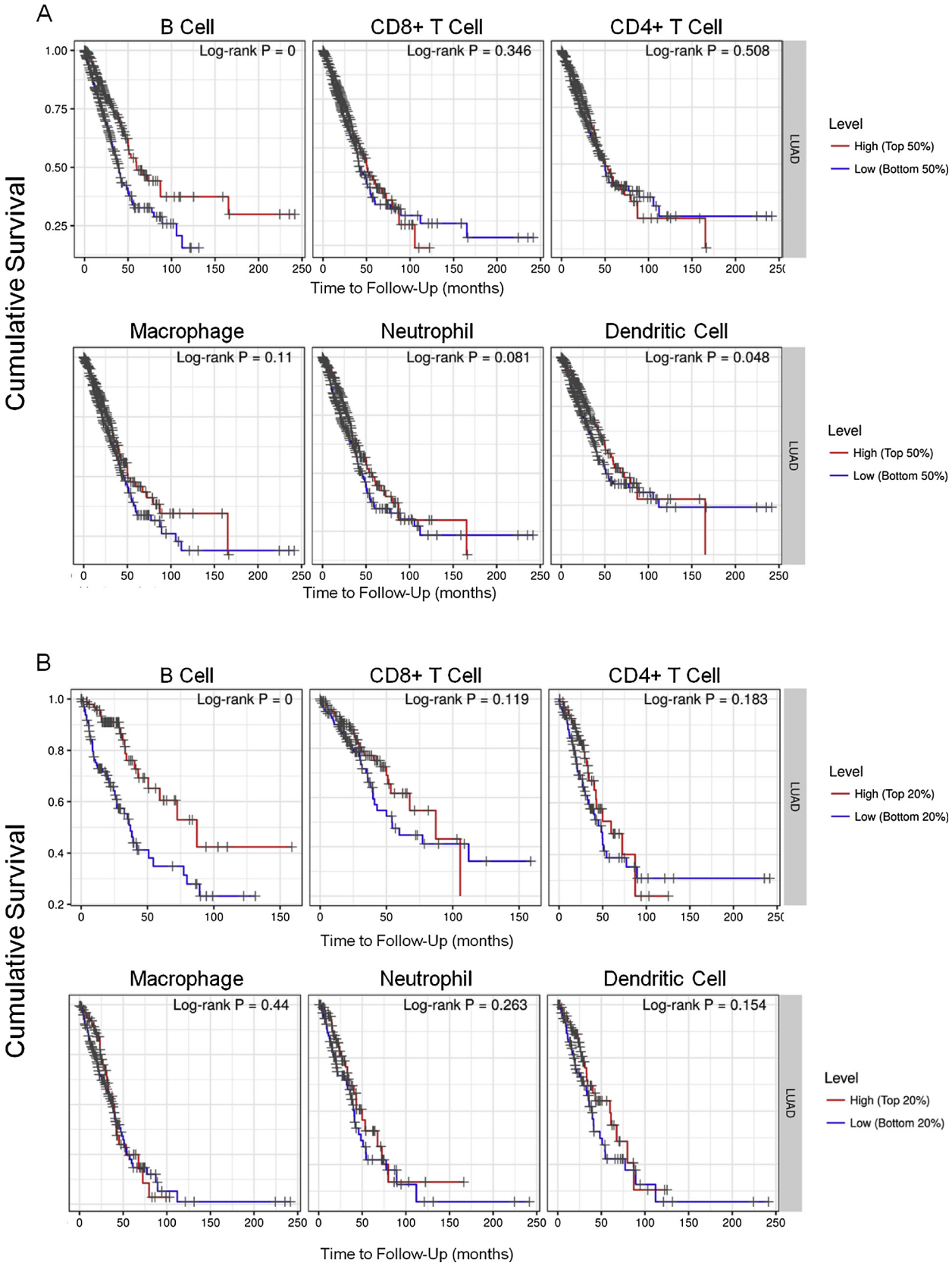

Fig. 3. Immune cell infiltration survival curve. In Fig. 3, A and B are K-M survival curves based on top and bottom sample partitions with 50% and 20% immune penetration, respectively. Red indicates high degree of infiltration and blue indicates low degree of infiltration. $p < 0.05$ was considered significant, and $P < 0.0001$ was represented by 0 (For interpretation of the references to colour in this figure legend, the reader is referred to the web version of this article).

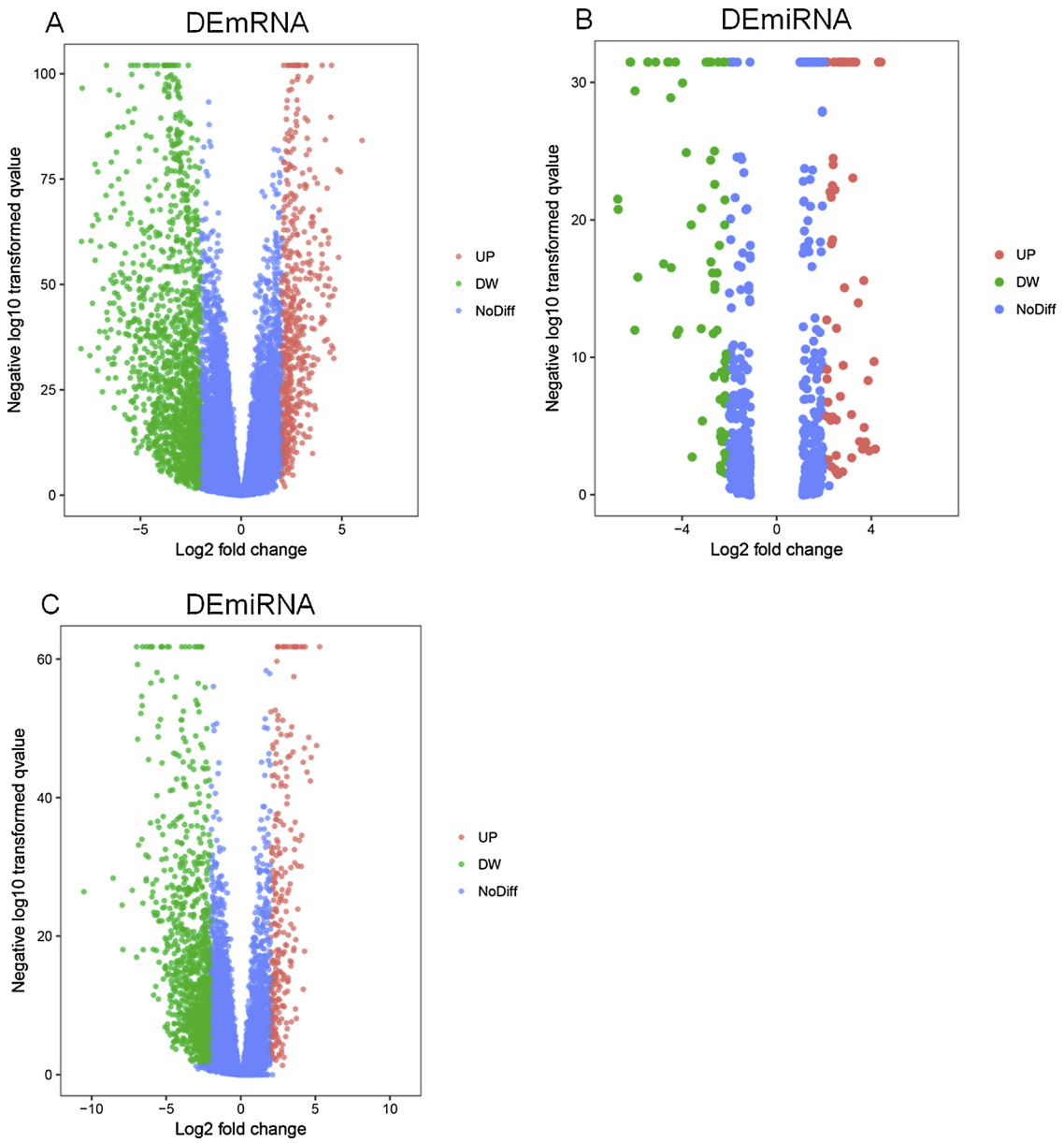

Fig. 4. Distribution of differential RNA. Fig. 4 shows the difference in expression of different RNAs in different samples. Red indicates significant upregulation in tumor samples, green indicates significant downregulation, and blue indicates no significant differences. Significant difference was determined by thresholding $|\log2\,FC| > 2$, $P < 0.05$ (For interpretation of the references to colour in this figure legend, the reader is referred to the web version of this article).

correlated with tumor purity are selected. To make the subsequent estimation more accurate, the TIMER algorithm removed the gene with the highest expression value in the previous step and used the constrained least-squares fit to estimate the infiltration abundance of the six immune cells [17]. The team of researchers integrated the TIMER algorithm and related results into an open source web tool called Tumor Immune Estimation Resource (TIMER; cistrome.shinyapps.io/timer), enabling researchers to study and visualize the relationship between tumor immune infiltration and disease [18].

2.4. The relationship between immune cell infiltration abundance and prognosis of LUAD

After assessing the abundance of immune infiltrating cells in each sample, we first studied the relationship between immune cell infiltration and LUAD prognosis. We performed univariate survival analysis on the infiltration abundance of six immune cells, plotted the K-M survival curve, and calculated the statistical significance. Then a multivariate Cox regression model adjusted for age, sex, tumor purity, stage, and viral infection status was used to construct a multivariate regression model of immune cell infiltration abundance to further explore the impact of immune infiltration on the prognosis of LUAD. The results showed that B cell infiltration was significantly associated with LUAD prognosis. The above method uses the TIMER server (https://cistrome.shinyapps.io/timer/) to complete.

2.5. B cell immune-related genes

Next, we screened mRNAs that are significantly associated with B cell infiltration. The expression pattern of these genes may play an important role in the LUAD immune response. We calculated the correlation between mRNA expression levels and B-cell infiltration abundance, using the Spearman correlation coefficient as a measure, and calculating the P value to test its statistical significance. $P < 0.01$, $R > 0.15$ were used as screening thresholds, and mRNAs that matched the conditions were considered as B cell immune related genes and

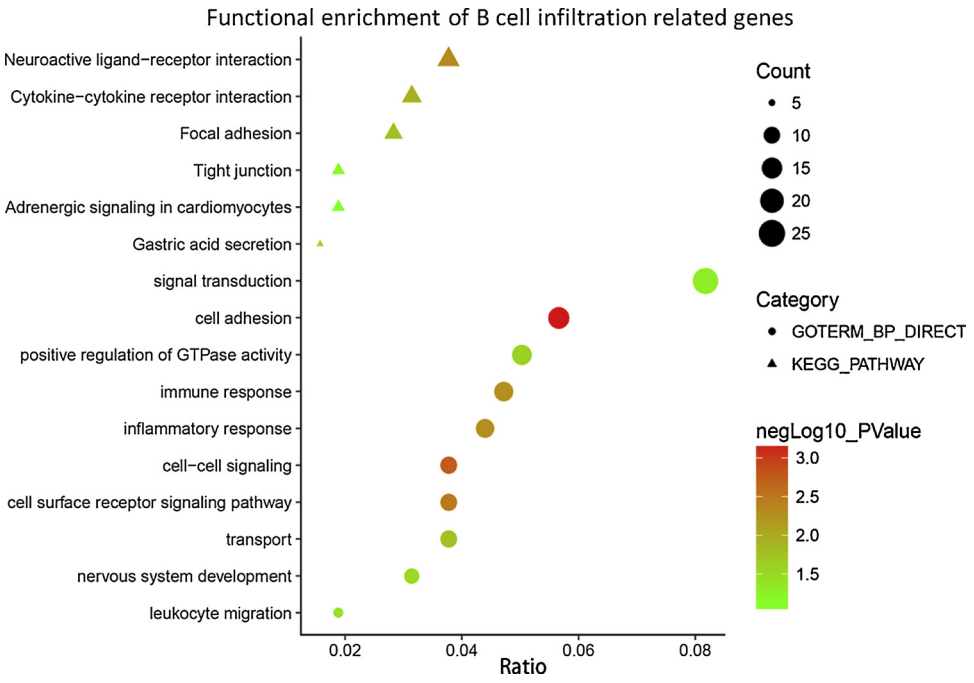

Fig. 5. Functional enrichment of B cell infiltration related genes. Fig. 5 shows the functional enrichment of 318 B cell immune related genes. The graph size represents the number of enriched genes, the graph type is used to distinguish between GO and KEGG analyses, the color represents the P value, the vertical axis represents the name of the relevant pathway and biological process, and the horizontal axis represents the percentage of the gene.

were included in subsequent studies.

2.6. Construction of immune-related ceRNA networks

For all differential lncRNAs (DElncRNAs) and differential miRNAs (DEmiRNAs), we discovered lncRNA-miRNA relationships by searching the miRcode (http://www.mircode.org/) database [19]. To find target genes for miRNAs in the network, 3p and 5p annotations of miRNAs were first performed via the starbase database [20]. For annotated miRNAs, miRNA-targeted mRNAs were searched in the miRDB, miRTarBase, TargetScan databases, respectively [21–23]. Only miRNA-mRNA Relationship Pairs Consistent with Three Databases Are Retained. To construct ceRNA networks associated with LUAD and B cell immune infiltration, we only retained differential mRNAs associated with B cell and screened pairs of mRNA-miRNA and lncRNA-miRNA. Finally, the visualization of ceRNA network was constructed using Cytoscape v3.6.0 software [24].

At the same time, our team used the improved NMF algorithm to predict the ceRNA network. The results are similar to the results of the proposed method in the key parts of the network. For our algorithm, it is elaborated in the forthcoming journal, doi:10.7150/ijbs.27555. The results are shown in Fig. 1 of the supplementary document. Since the algorithm only predicts the network and needs further biological verification, this paper directly uses the database to verify the relationship pairs to build the network, so the information obtained is what we need.

In order to verify our conjecture in many aspects, we performed WGCNA co-expression analysis on DElncRNA and DEmiRNA. WGCNA (weighted gene co-expression network analysis) is an analytical method for analyzing the expression patterns of multiple sample genes, which can be similar in expression pattern. The genes are clustered and analyzed for the association between modules and specific traits or phenotypes, and are therefore widely used in research on diseases and other traits and gene association analysis.

2.7. Statistical analysis

With regard to the exploration of the effect of immune infiltration on clinical outcomes, a multivariable Cox regression adjusted for infiltration abundance, age, gender, tumor purity, stage, and viral infection status was constructed using a TIMER server [18]. Univariate COX analysis was performed on 318 immune-related genes, and mRNA with a significance level of less than 0.0001 was screened as a clinically relevant gene. Then use clinically relevant genes to build a multi-factor COX risk proportional regression model based on maximum information volume. This model is a semi-parametric regression model proposed by British statistician D.R.Cox (1972) [25]. The model uses survival outcomes and survival time as dependent variables. It can simultaneously analyze the influence of many factors on the survival time, and can analyze the data with truncated survival time, and does not require the estimation of the survival distribution type of the data. Kaplan-Meier analysis was used to demonstrate the difference in 5-year overall survival (OS) and biomarker expression. The above analysis was implemented using the R package 'survival'. Other analyses, including Spearman correlation analysis and Wilcox rank sum test, were performed using R software [26].

2.8. Functional enrichment analysis

Functional enrichment analysis of B cell immune infiltration related genes was used to reveal the biological function of these genes in LUAD pathogenesis and immune regulation. The GO and KEGG analysis uses the online database DAVID v6.8 [27], and visual display through R software [26].

3. Result

3.1. Calculate immune cell infiltration

Using the LUAD gene expression profile (transcriptional reads per million readings (TPM)) from the TCGA as input data for the TIMER algorithm, the infiltration abundance of the six immune cells in each sample was fitted (Fig. 2, Table S1). The results showed that the infiltration abundance of immune cells in different types of tissue samples was significantly different, with B cell and CD4 T cells infiltrating in tumors, indicating that humoral immunity may play an important role in the LUAD immune response.

3.2. Prognostic relevance of immune cell infiltration in LUAD

We explored the relationship between immune cell infiltration and

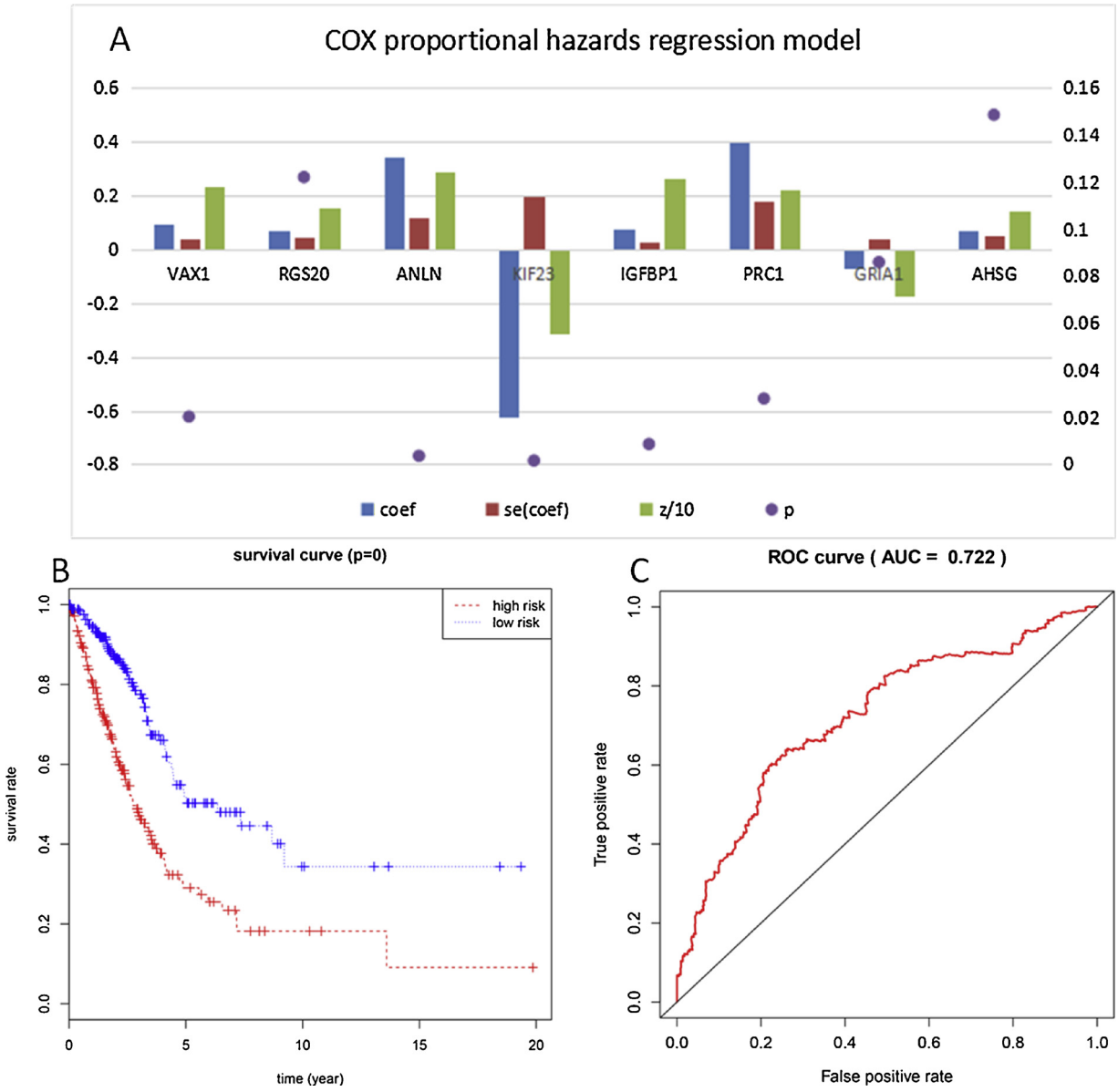

Fig. 6. Construction of COX Regression Model Using B Cell Infiltration Related Genes. Fig. 6A shows the model-related parameters. The P value is measured on the right vertical axis, and the remaining indicators are measured on the left vertical axis. Figure B shows the survival curve based on dividing the sample according to the median value of the risk value. Red indicates the high risk group and blue indicates the low risk group. Figure C shows the receiver operating characteristic (ROC) curve for this model (For interpretation of the references to colour in this figure legend, the reader is referred to the web version of this article).

LUAD prognosis. First, univariate survival analysis was performed for different immune cell infiltration and KM survival curve was drawn (Fig. 3). The results showed that the survival time of patients with high B cell infiltration was significantly higher than that of patients with low infiltration. Then we constructed a multivariate COX risk prognostic model related to immune infiltration (Table S2). By using multivariate COX regression adjusted for age, stage, viral infection, gender, and tumor purity, we determined the correlation between different immune cell infiltration abundances and LUAD prognosis. We found that infiltrating B cell were significantly associated with patient survival, and after adjustment for other covariates, it remained a good independent predictor. This shows that high B cell infiltration has a good effect on the survival of LUAD patients.

3.3. Difference analysis

We used the R package 'DESeq2' for the differential analysis of the original data downloaded from the TCGA to extract the LUAD-related differential mRNA (DEmRNA), differential lncRNA (DElncRNA) and differential miRNA (DEmiRNA). 2154 DEmRNAs (Table S3), 133 DEmiRNAs (Table S4), and 1474 DElncRNAs (Table S5) were extracted (Fig. 4).

3.4. B cell immune-related genes

We searched for genes related to B cell infiltration. The expression pattern of these genes may have an effect on prognosis by affecting LUAD immune infiltration. By calculating the Spearman correlation coefficient between gene expression values (TPM data) and immune infiltration abundance, we selected 318 genes from DEmRNA as B cell immune-related genes (Table S6). We first used the text mining method to verify the results. The facts showed that most of the (296) mRNAs obtained were related to the B-cells. We analyzed the survival information of these genes and found that 126 of them are significantly

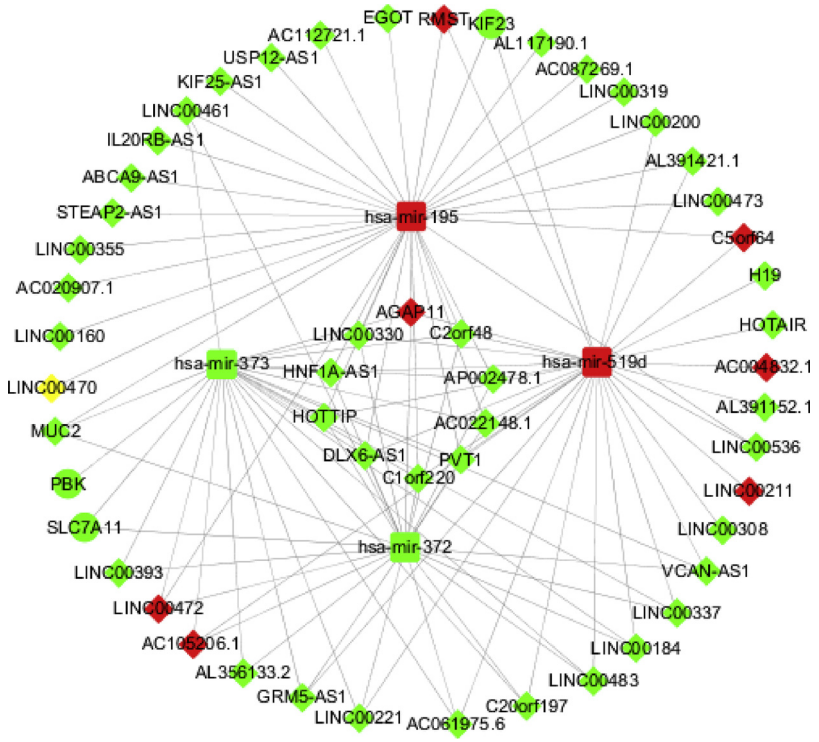

Fig. 7. B cell immune related ceRNA network. In Fig. 7, diamonds represent lncRNAs, rounds represent mRNAs, rectangles represent miRNAs, greens indicate down-regulation in cancer samples, and reds indicate up-regulations in cancer samples.

associated with prognosis. Then through functional enrichment analysis, we preliminary studied the role of these genes in biological functions and processes (Fig. 5). Enrichment analysis confirmed our hypothesis that these genes are closely related to B cell infiltration and play an important role in the LUAD immune response.

Next we explored how B cell immune-related genes influence clinical outcomes. A multivariate COX risk regression model with variable gene expression values was constructed (Fig. 6). The model used eight gene expression values as variables (Fig. 6A), reflecting the effect of gene expression values on LUAD production, with high-risk and low-risk groups showing significant differences in survival time (Fig. 6B). Among the eight variables, the expression values of five genes (*VAX1, ANLN, KIF23, IGFBP1, PRC1*) can be used as LUAD independent prognostic factors. The expression values of these genes interact with B cell infiltration, which affects the tumor microenvironment and affects the tumor immune effect of patients.

We performed WGCNA co-expression analysis of differential miRNAs and lncRNAs in key pathways, and the results confirmed the ceRNA network we constructed to some extent (supplementary Fig. 2).

3.5. Construction of ceRNA network related to B cell immune infiltration

To explore the intrinsic mechanism of LUAD immunological heterogeneity, we constructed a ceRNA network (Fig. 6). As the results of the above studies show that B cell infiltration is highly correlated with the prognosis of LUAD, we chose only B cell infiltration related genes as the basis for constructing the network. In this way, the underlying pathogenic mechanism of LUAD and the RNA molecules related to the results of immunotherapy are discovered. Through the database search of DElncRNA and DEmiRNA, we obtained 489 lncRNA-miRNA relationships (Table S7), of which 23 were miRNAs and 120 were lncRNAs. For 23 miRNAs, we searched for their target genes and found 1177 miRNA-mRNA pairs (Table S8). There were 921 mRNAs and 21 miRNAs. We searched for mRNAs related to B cell infiltration in these mRNAs and obtained three key genes (*KIF23*, *PBK*, and *SLC7A11*) to construct a B cell immune-related ceRNA network (Fig. 7). The network contains 3 mRNAs, 4 miRNAs, and 50 lncRNAs. The interaction between RNA molecules in this network may play an important regulatory role in the LUAD immune response. The key molecules in the network are our next key research goals. These RNAs may be potential immunotherapeutic targets.

We first performed a Kaplan-Meier survival curve and a log-rank test on the RNA in the network. The results showed that most of the RNA was significantly associated with the prognosis of LUAD. In this network, 10 lncRNAs and 3 mRNAs were significantly associated with survival (Fig. 8). Interestingly, *KIF23* in the network is a key prognostic factor for our previously constructed COX risk proportional regression model, suggesting that *KIF23* may play an important role in the immune response and prognosis of LUAD (Fig. 9). We performed a survival analysis of *KIF23* and explored its relationship with immune cell infiltration and tumor purity. The results showed that patients with different *KIF23* expression values showed significant differences in survival time, and low expression of *KIF23* predicted a higher survival time. The expression of *KIF23* seems to have a significant correlation with B cell infiltration, which also validates our previous conjecture.

To verify the reliability of the database, we performed co-expression analysis of DElncRNA and DEmiRNA (Supplementary Document Fig. 2). The results show that multiple pairs of lncRNA-miRNAs appear in the same module and are nodes in our network. It is suggested that the molecules in the network we construct may affect the relevant pathways of LUAD and thus play a role in tumor immune response.

We conducted a correlation analysis of potential mRNA-lncRNA competition relationships in the network and found multiple pairs of positively related RNAs (Fig. 10), suggesting that there may be competing relationships among these RNA pairs and validating the rationality of the ceRNA hypothesis. The interaction between RNAs in the network we constructed became a key factor in the LUAD immune process, affecting the infiltration of B cells in LUAD tumors and the prognosis of patients.

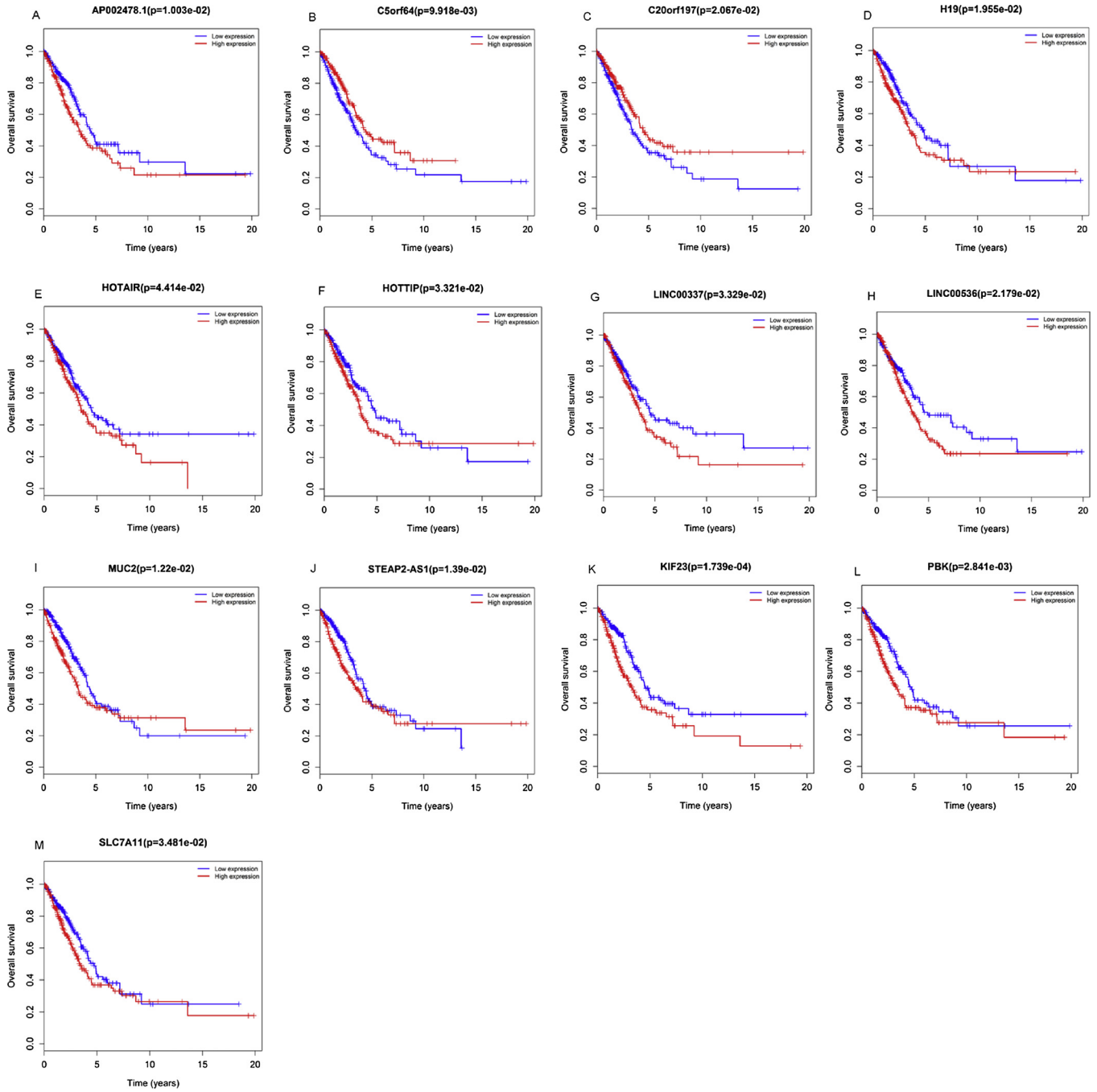

Fig. 8. Survival curves of RNAs in the network. In the ceRNA network, the survival curve of the RNAs significantly correlated with survival, $p < 0.05$ was considered statistically significant.

4. Discussion

In recent years, tumor immunotherapy has achieved remarkable results in clinical practice. However, considering the different patterns of tumor-infiltrating lymphocytes, individuals respond significantly differently after immunotherapy. The interaction of the tumor with its microenvironment is crucial in the development and prognosis of the tumor. For example, previous studies have shown that the number of B cell is a key factor in tumor immunity, is associated with a longer survival time, and has a dual effect on tumor recurrence and progression [28]. Whereas CD8 + T cells are associated with better overall survival and fewer relapses, macrophages are associated with worse clinical outcomes for many cancer types [8]. Therefore, the evaluation of tumor-infiltrating lymphocytes (TIL) is crucial in the study of cancer immunotherapy. Our study used the TIMER algorithm to assess the infiltration abundance of six immune cells in different samples. Based on this, an immune-related ceRNA network was constructed and the effects of competitive regulation of different RNAs on LUAD immune response and clinical outcome were analyzed.

Compared to previous methods, the TIMER algorithm not only uses selected tag genes to eliminate the effect of highly expressed genes on the deconvolution results, but also evaluates six immune cell infiltration abundances, eliminating cells with similar expression patterns. The effect of collinearity on the regression results. TIMER is superior to previous algorithms in accuracy and so on. After TIMER was used for TIL assessment, we analyzed the effects of different immune penetrations in the clinic. The results showed that high B cell infiltration predicts better survival and B cell infiltration plays an important role in

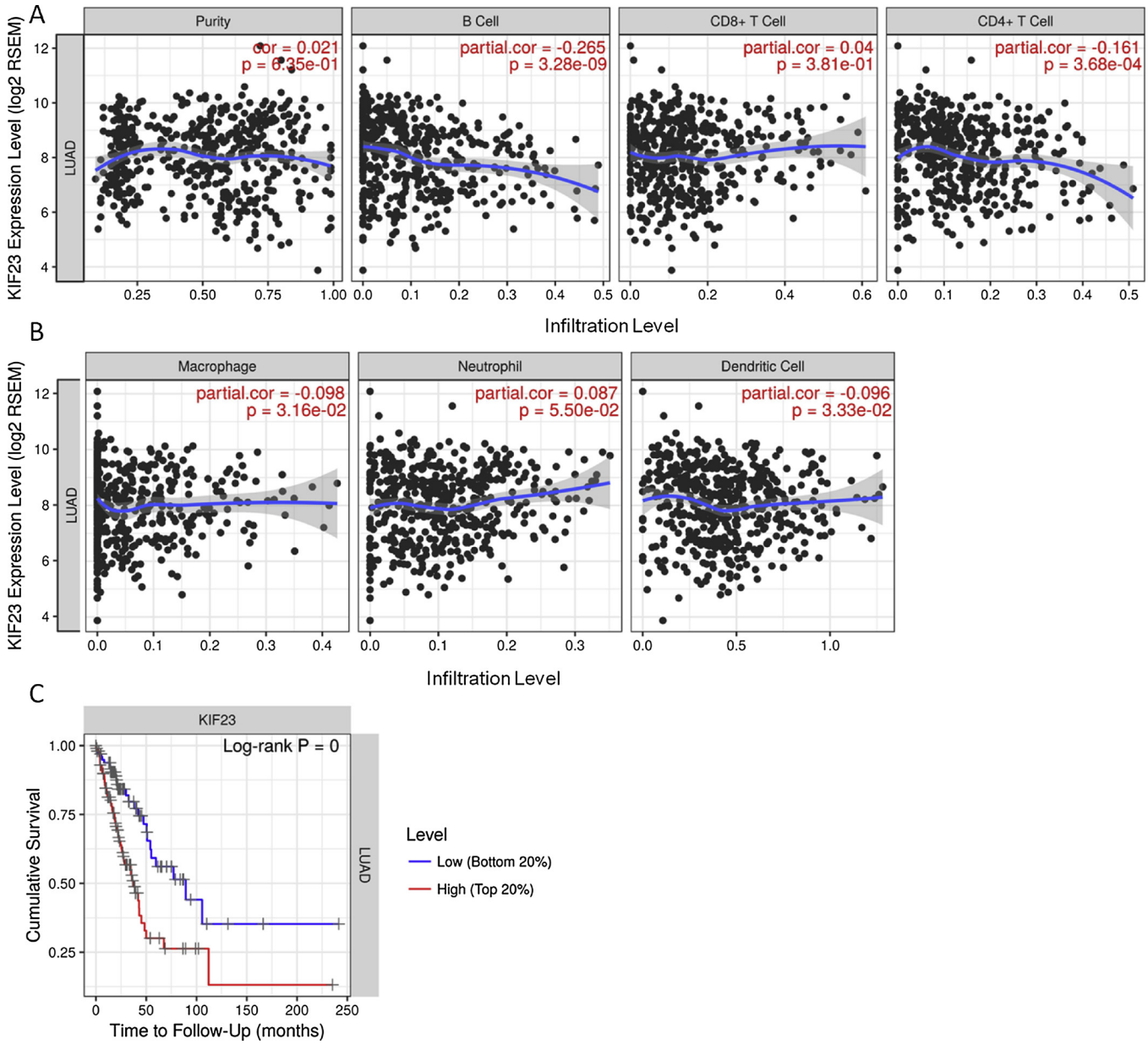

Fig. 9. Association of *KIF23* with Immune Response. Fig. 9A and B show the correlation between the immuno-infiltration abundance and the *KIF23* expression value. The abscissa indicates the abundance of infiltration and the ordinate indicates the gene expression value (log2 RSEM). Different subgraphs indicate tumor purity and six different immune cells. $P < 0.05$ was considered statistically significant. Fig. 10C shows the survival curves of patients with *KIF23* expression in the top 20% and bottom 20%. Red indicates top 20%, blue indicates bottom 20% (For interpretation of the references to colour in this figure legend, the reader is referred to the web version of this article).

LUAD immunity, which is consistent with previous studies [29,30]. Therefore, through correlation analysis, we identified 318 genes that were significantly associated with B cell infiltration in LUAD differential genes and performed bioinformatics analysis. The results show that most of these genes are involved in tumor immunity and may play an important role in the prognosis of patients. Using multivariate COX regression analysis, we selected eight mRNA expression values (including *KIF23*) as variables and constructed a survival regression model to predict the relationship between gene expression and patient survival.

In order to further explore the regulatory mechanisms of B cell infiltration at the RNA molecule level, we constructed a ceRNA network associated with B cell immune infiltration. In this network, three key mRNAs (*PBK*, *KIF23* and *SLC7A11*) were shown to be significantly associated with survival, and in many studies they have been shown to play an important role in cancer and immunity. *PBK* plays a role in the activation of B lymphocytes. Related studies have shown that *PBK* is associated with mutant p53 and affects lung adenocarcinoma cell proliferation, viability, and prognosis. *PBK* can also stabilize Nrf2, strictly regulate ROS levels, promote cell cycle progression, and inhibit apoptosis, and promote promyelocytic proliferation [31,32]. In advanced lung cancer and primary lung tumors, *KIF23* transcripts are overexpressed in the vast majority of metastatic lymph nodes. Inhibition of *KIF23* expression effectively inhibits the growth of lung cancer cells [33]. *SLC7A11* is a gene encoding the cystine-glutamate transporter that has been detected in various cancers. Overexpression of *SLC7A11* may be an unfavorable prognostic factor and may be a potential therapeutic target for liver cancer [34].

For the miRNAs in the network (*hsa-mir-195, hsa-mir-372d, hsa-mir-372* and *hsa-miR-373*), their role in tumor immunity is also crucial. The

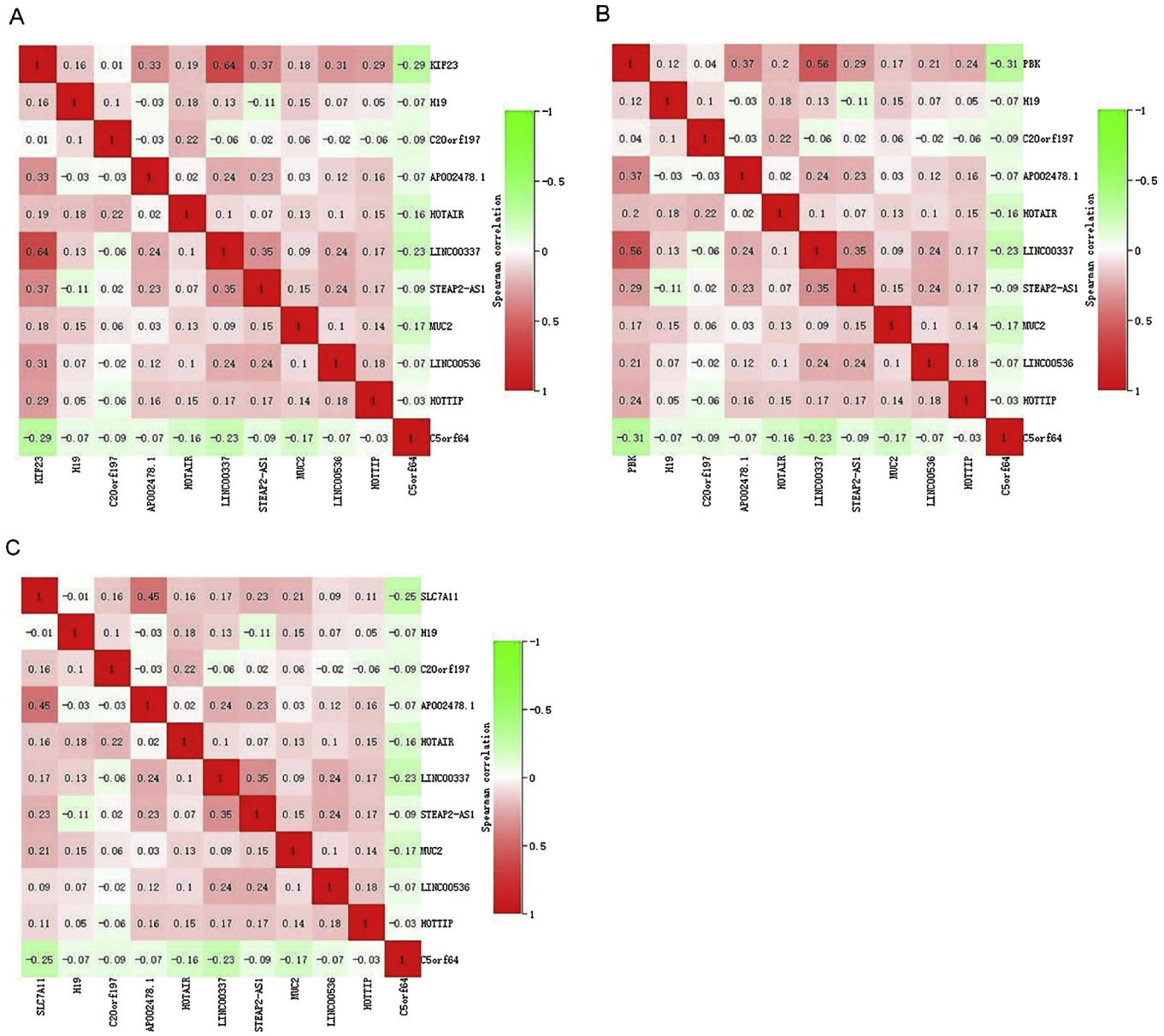

Fig. 10. Correlation in ceRNA networks. Fig. 10A-C show the correlation of mRNA (*KIF23*, *PBK*, and *SLC7A11*) expression values in the ceRNA network and lncRNA expression values with which they are potentially competing with each other.

high expression of *hsa-mir-195* can inhibit tumor growth and has a good survival rate in many malignant tumors including non-small cell lung cancer [35]. Related studies have shown that *hsa-mir-519d* plays an important role in gastric cancer [36]. *Hsa-mir-195* is associated with the proliferation and metastasis of cancer cells in various cancers (liver cancer, kidney cancer, head and neck squamous cell carcinoma), and is significantly associated with the prognosis of oral cancer and liver cancer [37–41]. In addition, *hsa-mir-195* expression is abnormal in childhood B-cell precursor acute lymphoblastic leukemia [42]. Ten lncRNAs in the network were also significantly associated with survival in patients with LUAD. Among them, *AP002478.1*, *C20orf197*, *HOTTIP*, *LINC00337* and *MUC2* interact with multiple miRNAs and mRNAs in the ceRNA network. Our study showed a significant positive correlation between the expression of *LINC00337* and *KIF23*, *PBK*, *AP002478.1*, and *SLC7A11*. This suggests that *LINC00337* may affect the expression of *PBK* and *KIF23* through competitive binding of *has-mir-373* and *has-mir-519d*. *AP002478.1* competitive binding *has-mir-373* and *has-mir-372* affect the expression of *SLC7A11*. Therefore, the critical RNA in the network we construct may have an important impact on the outcome of immunotherapy and can be used as a potential biomarker for immunotherapy.

Funding

This work was supported by the National Natural Science Foundation of China (No. 61271446) Natural Science Foundation of Shanghai (No. 18ZR1417200) National Natural Science Foundation of China (No. 61803257).

Competing interests

The authors declare no conflict of interests.

Appendix A. Supplementary data

Supplementary material related to this article can be found, in the online version, at doi:https://doi.org/10.1016/j.prp.2018.10.032.

References

[1] D.M. Pardoll, The blockade of immune checkpoints in cancer immunotherapy, Nat. Rev. Cancer (2012), https://doi.org/10.1038/nrc3239.

[2] P. Sharma, K. Wagner, J.D. Wolchok, J.P. Allison, Novel cancer immunotherapy agents with survival benefit: recent successes and next steps, Nat. Rev. Cancer (2011), https://doi.org/10.1038/nrc3153.

[3] A.M. Di Giacomo, L. Calabrò, R. Danielli, E. Fonsatti, E. Bertocci, I. Pesce, C. Fazio, O. Cutaia, D. Giannarelli, C. Miracco, M. Biagioli, M. Altomonte, M. Maio, Long-term survival and immunological parameters in metastatic melanoma patients who responded to ipilimumab 10 mg/kg within an expanded access programme, Cancer immunol. Immunother. (2013), https://doi.org/10.1007/s00262-013-1418-6.

[4] P.A. Prieto, J.C. Yang, R.M. Sherry, M.S. Hughes, U.S. Kammula, D.E. White, C.L. Levy, S.A. Rosenberg, G.Q. Phan, CTLA-4 blockade with ipilimumab: long-term follow-up of 177 patients with metastatic melanoma, Clin. Cancer Res. (2012), https://doi.org/10.1158/1078-0432.CCR-11-1823.

[5] X.S. Liu, E.R. Mardis, Applications of immunogenomics to cancer, Cell (2017), https://doi.org/10.1016/j.cell.2017.01.014.

[6] M.S. Rooney, S.A. Shukla, C.J. Wu, G. Getz, N. Hacohen, Molecular and genetic properties of tumors associated with local immune cytolytic activity, Cell (2015), https://doi.org/10.1016/j.cell.2014.12.033.

[7] M. Angelova, P. Charoentong, H. Hackl, M.L. Fischer, R. Snajder, A.M. Krogsdam, M.J. Waldner, G. Bindea, B. Mlecnik, J. Galon, Z. Trajanoski, Characterization of the immunophenotypes and antigenomes of colorectal cancers reveals distinct tumor escape mechanisms and novel targets for immunotherapy, Genome Biol. 16 (2015) 64, https://doi.org/10.1186/s13059-015-0620-6.

[8] B. Li, E. Severson, J.C. Pignon, H. Zhao, T. Li, J. Novak, P. Jiang, H. Shen, J.C. Aster, S. Rodig, S. Signoretti, J.S. Liu, X.S. Liu, Comprehensive analyses of tumor immunity: implications for cancer immunotherapy, Genome Biol. (2016), https://doi.org/10.1186/s13059-016-1028-7.

[9] A.M. Newman, C.L. Liu, M.R. Green, A.J. Gentles, W. Feng, Y. Xu, C.D. Hoang, M. Diehn, A.A. Alizadeh, Robust enumeration of cell subsets from tissue expression profiles, Nat. Methods (2015), https://doi.org/10.1038/nmeth.3337.

[10] Y. Şenbabaoglu, R.S. Gejman, A.G. Winer, M. Liu, E.M. Van Allen, G. de Velasco, D. Miao, I. Ostrovnaya, E. Drill, A. Luna, N. Weinhold, W. Lee, B.J. Manley, D.N. Khalil, S.D. Kaffenberger, Y. Chen, L. Danilova, M.H. Voss, J.A. Coleman, P. Russo, V.E. Reuter, T.A. Chan, E.H. Cheng, D.A. Scheinberg, M.O. Li, T.K. Choueiri, J.J. Hsieh, C. Sander, A.A. Hakimi, Erratum to: Tumor immune microenvironment characterization in clear cell renal cell carcinoma identifies prognostic and immunotherapeutically relevant messenger RNA signatures [Genome Biology. 17, (2016) (231)] DOI: https://doi.org/10.1186/s13059-016-1092-z, Genome Biol. (2017). https://doi.org/doi:10.1186/s13059-017-1180-8.

[11] N. Rna, A. Fatica, I. Bozzoni, Long non-coding RNAs: new players in cell differentiation and development, Nat. Rev. Genet. (2014), https://doi.org/10.1038/nrg3606.

[12] M.K. Atianand, D.R. Caffrey, K.A. Fitzgerald, Immunobiology of long noncoding RNAs, Annu. Rev. Immunol. (2017), https://doi.org/10.1146/annurev-immunol-041015-055459.

[13] L. Salmena, L. Poliseno, Y. Tay, L. Kats, P.P. Pandolfi, A ceRNA hypothesis: The rosetta stone of a hidden RNA language? Cell (2011), https://doi.org/10.1016/j.cell.2011.07.014.

[14] M.I. Love, W. Huber, S. Anders, Moderated estimation of fold change and dispersion for RNA-seq data with DESeq2, Genome Biol. (2014), https://doi.org/10.1186/s13059-014-0550-8.

[15] B. Li, J.Z. Li, A general framework for analyzing tumor subclonality using SNP array and DNA sequencing data, Genome Biol. (2014), https://doi.org/10.1186/s13059-014-0473-4.

[16] C. Chen, K. Grennan, J. Badner, D. Zhang, E. Gershon, L. Jin, C. Liu, Removing batch effects in analysis of expression microarray data: an evaluation of six batch adjustment methods, PLoS One (2011), https://doi.org/10.1371/journal.pone.0017238.

[17] A.R. Abbas, K. Wolslegel, D. Seshasayee, Z. Modrusan, H.F. Clark, Deconvolution of blood microarray data identifies cellular activation patterns in systemic lupus erythematosus, PLoS One (2009), https://doi.org/10.1371/journal.pone.0006098.

[18] T. Li, J. Fan, B. Wang, N. Traugh, Q. Chen, J.S. Liu, B. Li, X.S. Liu, TIMER: a web server for comprehensive analysis of tumor-infiltrating immune cells, Cancer Res. (2017), https://doi.org/10.1158/0008-5472.CAN-17-0307.

[19] A. Jeggari, D.S. Marks, E. Larsson, miRcode: A map of putative microrna target sites in the long non-coding transcriptome, Bioinformatics. (2012), https://doi.org/10.1093/bioinformatics/bts344.

[20] J.H. Li, S. Liu, H. Zhou, L.H. Qu, J.H. Yang, StarBase v2.0: decoding miRNA-ceRNA, miRNA-ncRNA and protein-RNA interaction networks from large-scale CLIP-Seq data, Nucleic Acids Res. (2014), https://doi.org/10.1093/nar/gkt1248.

[21] V. Agarwal, G.W. Bell, J.W. Nam, D.P. Bartel, Predicting effective microRNA target sites in mammalian mRNAs, Elife (2015), https://doi.org/10.7554/eLife.05005.

[22] C.H. Chou, S. Shrestha, C.D. Yang, N.W. Chang, Y.L. Lin, K.W. Liao, W.C. Huang, T.H. Sun, S.J. Tu, W.H. Lee, M.Y. Chiew, C.S. Tai, T.Y. Wei, T.R. Tsai, H.T. Huang, C.Y. Wang, H.Y. Wu, S.Y. Ho, P.R. Chen, C.H. Chuang, P.J. Hsieh, Y.S. Wu, W.L. Chen, M.J. Li, Y.C. Wu, X.Y. Huang, F.L. Ng, W. Buddhakosai, P.C. Huang, K.C. Lan, C.Y. Huang, S.L. Weng, Y.N. Cheng, C. Liang, W.L. Hsu, H. Da Huang, MiRTarBase update 2018: a resource for experimentally validated microRNA-target interactions, Nucleic Acids Res. (2018), https://doi.org/10.1093/nar/gkx1067.

[23] N. Wong, X. Wang, miRDB: an online resource for microRNA target prediction and functional annotations, Nucleic Acids Res. (2015), https://doi.org/10.1093/nar/gku1104.

[24] P. Shannon, A. Markiel, O. Ozier, N.S. Baliga, J.T. Wang, D. Ramage, N. Amin, B. Schwikowski, T. Ideker, Cytoscape: a software Environment for integrated models of biomolecular interaction networks, Genome Res. (2003), https://doi.org/10.1101/gr.1239303.

[25] J. Fox, Cox Proportional-Hazards Regression for Survival Data The Cox Proportional-Hazards Model, Most (2002). doi:10.1016/j.carbon.2010.02.029.

[26] R. R Development Core Team, R: A Language and Environment for Statistical Computing, (2011), https://doi.org/10.1007/978-3-540-74686-7.

[27] D.W. Huang, B.T. Sherman, R.A. Lempicki, Bioinformatics enrichment tools: paths toward the comprehensive functional analysis of large gene lists, Nucleic Acids Res. (2009), https://doi.org/10.1093/nar/gkn923.

[28] G. Bindea, B. Mlecnik, M. Tosolini, A. Kirilovsky, M. Waldner, A.C. Obenauf, H. Angell, T. Fredriksen, L. Lafontaine, A. Berger, P. Bruneval, W.H. Fridman, C. Becker, F. Pagès, M.R. Speicher, Z. Trajanoski, J.Ô. Galon, Spatiotemporal dynamics of intratumoral immune cells reveal the immune landscape in human cancer, Immunity (2013), https://doi.org/10.1016/j.immuni.2013.10.003.

[29] D.J. DiLillo, K. Yanaba, T.F. Tedder, B cells are required for optimal CD4+ and CD8+ T cell tumor immunity: therapeutic B cell depletion enhances B16 melanoma growth in mice, J. Immunol. (2010), https://doi.org/10.4049/jimmunol.0903009.

[30] C. Germain, S. Gnjatic, F. Tamzalit, S. Knockaert, R. Remark, J. Goc, A. Lepelley, E. Becht, S. Katsahian, G. Bizouard, P. Validire, D. Damotte, M. Alifano, P. Magdeleinat, I. Cremer, J.L. Teillaud, W.H. Fridman, C. Sautès-Fridman, M.C. Dieu-Nosjean, Presence of B cells in tertiary lymphoid structures is associated with a protective immunity in patients with lung cancer, Am. J. Respir. Crit. Care Med. (2014), https://doi.org/10.1164/rccm.201309-1611OC.

[31] B. Lei, W. Qi, Y. Zhao, Y. Li, S. Liu, X. Xu, C. Zhi, L. Wan, H. Shen, PBK/TOPK expression correlates with mutant p53 and affects patients' prognosis and cell proliferation and viability in lung adenocarcinoma, Hum. Pathol. (2015), https://doi.org/10.1016/j.humpath.2014.07.026.

[32] Y. Liu, H. Liu, H. Cao, B. Song, W. Zhang, W. Zhang, PBK/TOPK mediates promyelocyte proliferation via Nrf2-regulated cell cycle progression and apoptosis, Oncol. Rep. (2015), https://doi.org/10.3892/or.2015.4308.

[33] T. Kato, H. Wada, P. Patel, H.P. Hu, D. Lee, H. Ujiie, K. Hirohashi, T. Nakajima, M. Sato, M. Kaji, K. Kaga, Y. Matsui, M.S. Tsao, K. Yasufuku, Overexpression of KIF23 predicts clinical outcome in primary lung cancer patients, Lung Cancer. (2016), https://doi.org/10.1016/j.lungcan.2015.11.018.

[34] M.D. Polewski, R.F. Reveron-Thornton, G.A. Cherryholmes, G.K. Marinov, K.S. Aboody, *SLC7A11* overexpression in glioblastoma is associated with increased Cancer stem cell-like properties, Stem Cells Dev. (2017), https://doi.org/10.1089/scd.2017.0123.

[35] B. Liu, J. Qu, F. Xu, Y. Guo, Y. Wang, H. Yu, B. Qian, MiR-195 suppresses non-small cell lung cancer by targeting CHEK1, Oncotarget (2015), https://doi.org/10.18632/oncotarget.3255.

[36] X.W. Wang, Y. Wu, D. Wang, Z.F. Qin, Microrna network analysis identifies key micrornas and genes associated with precancerous lesions of gastric cancer, Genet. Mol. Res. (2014), https://doi.org/10.4238/2014.October.27.10.

[37] J. An, J. Xu, J. Li, S. Jia, X. Li, Y. Lu, Y. Yang, Z. Lin, X. Xin, M. Wu, Q. Zheng, H. Pu, X. Gui, T. Li, D. Lu, HistoneH3 demethylase JMJD2A promotes growth of liver cancer cells through up-regulating miR372, Oncotarget 8 (2017) 49093–49109, https://doi.org/10.18632/oncotarget.17095.

[38] H. Chen, Z. Zhang, Y. Lu, K. Song, X. Liu, F. Xia, W. Sun, Downregulation of ULK1 by microRNA-372 inhibits the survival of human pancreatic adenocarcinoma cells, Cancer Sci. (2017), https://doi.org/10.1111/cas.13315.

[39] X. Huang, M. Huang, L. Kong, Y. Li, miR-372 suppresses tumour proliferation and invasion by targeting IGF2BP1 in renal cell carcinoma, Cell Prolif. (2015), https://doi.org/10.1111/cpr.12207.

[40] Q. Wang, S. Liu, X. Zhao, Y. Wang, D. Tian, W. Jiang, MiR-372-3p promotes cell growth and metastasis by targeting FGF9 in lung squamous cell carcinoma, Cancer Med. 6 (2017) 1323–1330, https://doi.org/10.1002/cam4.1026.

[41] G. Wu, Y. Wang, X. Lu, H. He, H. Liu, X. Meng, S. Xia, K. Zheng, B. Liu, Low mir-372 expression correlates with poor prognosis and tumor metastasis in hepatocellular carcinoma, BMC Cancer (2015), https://doi.org/10.1186/s12885-015-1214-0.

[42] X. Ju, D. Li, Q. Shi, H. Hou, N. Sun, B. Shen, Differential microRNA expression in childhood B-cell precursor acute lymphoblastic leukemia, Pediatr. Hematol. Oncol. (2009), https://doi.org/10.1080/08880010802378338.